Nanostructured, Molecularly Imprinted, and Template-Patterned Polythiophenes for Chiral Sensing and Differentiation

*Roderick B. Pernites, Subrahmanyam K. Venkata, Brylee David B. Tiu, Allan Christopher C. Yago, and Rigoberto C. Advincula**

Molecular imprinting is a technique for making synthetic polymers with artificial molecular recognition sites specific for the imprinted molecule called the template, which then becomes the target analyte for detection.[1] Generally, the imprinting procedure involves polymerizing functionalized monomers with cross-linkers in the presence of the template molecule and with an initiator.[1] The subsequent extraction of the template from the polymer film creates complementary cavities (also called imprint sites) that contain the exact memory of the size, shape, and functional group orientation of the original template in 3D space.

The molecular imprinting technique has origins from the seminal work of Polyakov in 1931,[2] in which the silica particles were observed to have unusual adsorption properties selective to the imprinted additives compared even to structurally related compounds. Although the pioneering work was started by Polyakov, molecular imprinting or molecularly imprinted polymers (MIP) was popularized by Mosbach, Shea, and Wulff.[3] To date, most MIPs are prepared as bulk monolith via free radical polymerization.[1a] However, these molecularly imprinted monoliths have been reported to have poor sensitivity and lack repeatable selectivity.[1] To resolve these perennial challenges, MIPs have been prepared as thin films, which is a major direction in molecular imprinting technology. Recently, our group has reported a simple approach of creating MIP sensor films using anodic and cathodic electrodeposition[4,5,7–9] and self-assembly[6] process for targeting various analytes such as folic acid,[4] bis-phenol A,[5] dinitrotoluene,[6] dopamine,[7] theophylline,[8] naproxen,[9] and paracetamol.[9] With the anodic electrodeposition approach, we introduced the use of a single functional and cross-linking monomer without employing a separate cross-linker and initiator for fabricating an MIP film that is directly interfaced onto sensor transducers, particularly quartz crystal microbalance (QCM)[4,6] and surface plasmon resonance (SPR) spectroscopy.[7–9]

In this communication, we report, for the first time electropolymerized MIP films with nanopatterned morphology using latex colloidal particles as sacrificial templates for sensing. Briefly, the method (**Scheme 1**) involves 1) colloidal sphere layering of latex particles onto the surface via Langmuir–Blodgett (LB)-like technique[10] followed by 2) noncovalent molecular imprinting of the template analyte using cyclic voltammetric (CV) electrodeposition of a single functional and cross-linking terthiophene monomer derivative with a carboxylic acid moiety (G0-3TCOOH). Previously, we have shown that the LB-like technique allows the monolayer ordering of polystyrene particles in hexagonal close packing arrangement onto conducting electrode surfaces.[11]

This new technique of assembling electropolymerized MIP film addresses some of the shortcomings of the earlier MIP preparation methods in relation to thickness. For instance, in a thick MIP film, template removal is difficult and its rebinding is slow because the cavities are deeply buried into the polymer film. However, in the case of a thin MIP film, the template loading into the film is closer to the subphase/transducer interface, and thus less template analyte need to be rebinded and detected. Thus with the electropolymerized and colloidally templated MIP film, template molecules are imprinted to form cavities closer to the solution subphase and at a higher surface/volume ratio.

Furthermore, in this report, the fabricated colloidally templated and nanostructured electropolymerized MIP film enabled the sensing and differentiation of a chiral compound i.e., (–)-and (+)-norephedrine (model template) diastereomers, which is rare and difficult to attain using earlier MIP films. Norephedrine is a member of the Ephedrine alkaloids, which are considered naturally occuring chemical stimulants that are added in dietary supplements to enhance athletic

Dr. R. B. Pernites
Department of Chemical and Biomolecular Engineering Rice University
MS 362, 6100 Main Street, Houston, TX, 77005, USA
S. K. Venkata, B. D. B. Tiu, A. C. C. Yago, Prof. R. C. Advincula
Department of Chemistry and Department of Chemical and Biomolecular Engineering
University of Houston
Houston, TX 77204-5003, USA
E-mail: rca41@case.edu; radvincula@uh.edu
Prof. R. C. Advincula
Department of Macromolecular Science and Engineering
Case Western Reserve University
Cleveland, OH 44106, USA

DOI: 10.1002/smll.201102331

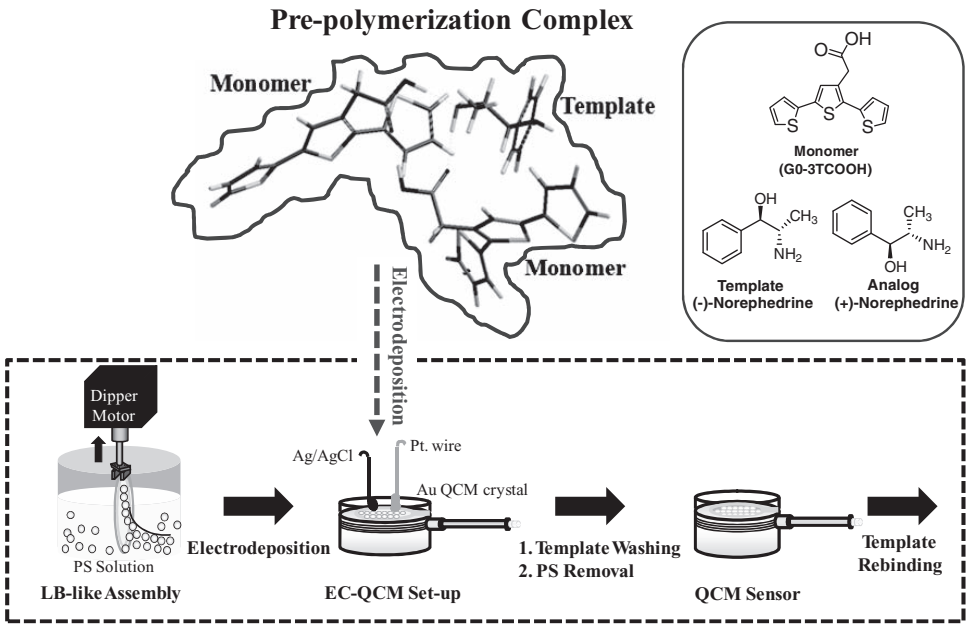

Scheme 1. Fabrication of molecularly imprinted and templated polythiophene sensor film onto QCM: 1) PS layering from SDS-PS solution, 2) CV electrodeposition of the MIP solution, 3) template and PS removal, and 4) template analyte sensing. Top inset: Computer generated images of the 2D optimized structure (stick model) of the pre-polymerization complex[12] between the terthiophene monomer (G0-3TCOOH) and template (norephedrine) generated using semi-empirical AM1 quantum calculations.[13] Calculated complexation energy[4,8,13] of the pre-polymerization complex is about −25.14 kJ mol^{-1}. See Supporting Information (SI) for colored figures.

performance or to promote weight loss.[14] However, these supplements have been found to have many adverse health effects,[14] which actually led to the development of many analytical methods for the determination of Ephedrine alkaloids and eventually prohibition for their use in dietary supplement by the US Food and Drug Administration (FDA).[15] Norephedrine exists into two diastereomeric forms such as 1) (−)-(1*R*,2*S*)-norephedrine and 2) (+)-(1*S*,2*S*)-norephedrine also called norpseudoephedrine.[16]

Additionally, unlike our previous electropolymerized MIPs that use a QCM transduction,[4,6] a small commercially available QCM set-up is utilized in this study, which is portable and capable for on-site or field testing of different analytes. The two different QCM set-ups used are shown in the supporting document (Figure S1a, Supporting Information (SI)).

The formation of the MIP sensor film onto the gold (Au) QCM crystal pre-coated with single layer of PS (500 nm size) particles was observed in the electrochemistry QCM (or EC-QCM) kinetic measurements (**Figure 1**). This technique has been used by our group to study the in-situ formation and electrodeposition of conducting polymer films.[4,5,17] From the results, the CV diagram (Figure 1a) of the MIP film deposition depicts the typical reduction-oxidation (redox) peak of the polythiophene[11d] with an onset potential at 0.4 V. The mechanism for the electropolymerization of the terthiophene monomer is explained elsewhere.[18] Briefly, the anodic peak beyond 1.0 V in the first CV scan has been reported to be due to the formation of the terthiophene radical cation (called polaron), which is achieved by losing an electron in the neutral monomer species.[18] Then during the reverse scan (reduction process), the radical cation is expected to couple with another charged specie in a 2,5 linkage to form a dimer.[18] In the second CV cycle, a new oxidation peak appears at a relatively lower potential (between 0.6 and

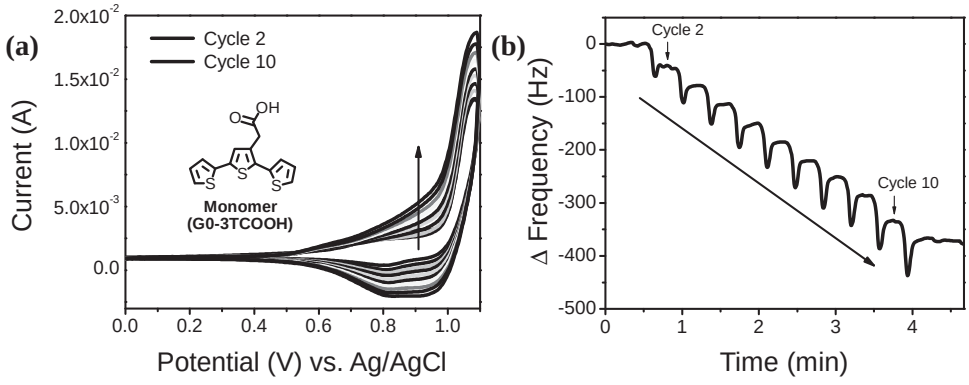

Figure 1. EC-QCM in-situ measurements of the CV electrodeposition of the MIP film onto PS- (500 nm size) templated Au surface: a) CV diagram and b) QCM response.

NANO MICRO small

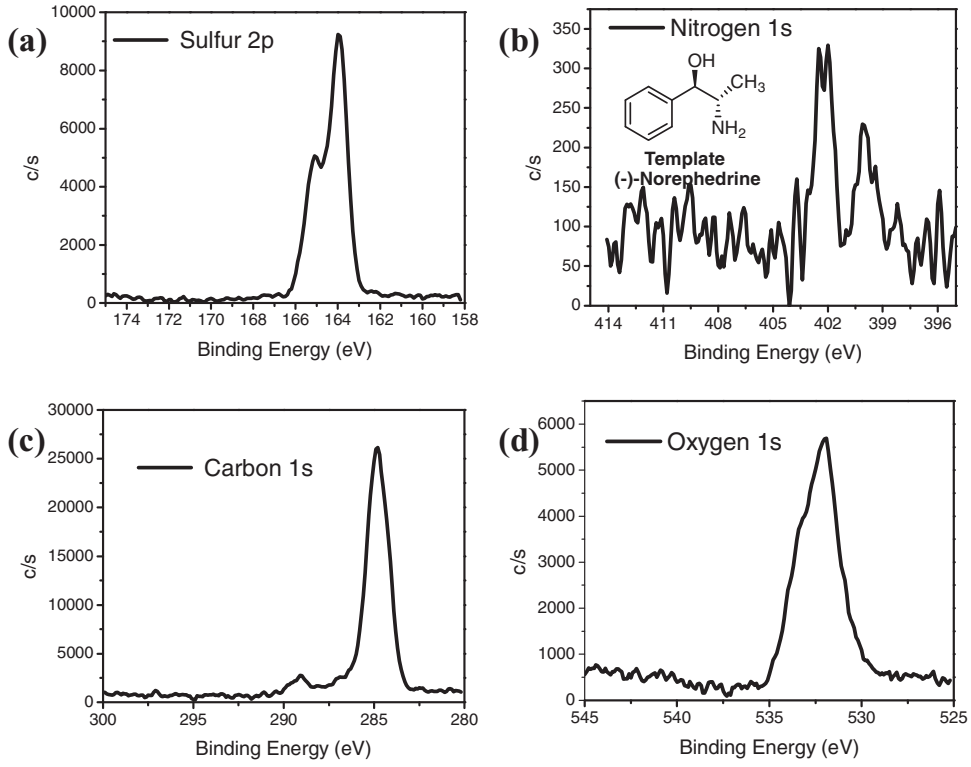

Figure 2. XPS high resolution scans of the molecularly imprinted and templated film (MIP) after PS removal and before template washing: a) sulfur 2p, b) nitrogen 1s, c) carbon 1s, and d) oxygen 1s.

1.0 V), which is related to the formation of a more stable dication (bipolaron) with extended π-conjugation that is easily oxidized compared to the radical cation.[18] Upon succeeding CV cycles until the 10th cycle, the current increases at this redox peak (between 0.6 and 1.0 V), indicating the formation of more conjugated species (oligomer and polymer) as a result of the further cross-linking between the terthiophene units and electrodeposition of the polymer film onto the Au QCM electrode substrate.[4,11d] The increase in the redox current in the CV diagram during the electrodeposition of the polythiophene film is accompanied by a change in frequency of the quartz crystal. Figure 1b depicts a recurring oscillation in the ΔF change of the QCM crystal for each CV cycle as the polythiophene film switches from oxidized to reduced states. Upon oxidation of the polymer (also called doping process), the ΔF decreases and then slightly increases upon reduction and eventually stabilizes at neutral state (0 V). During doping, the polymer becomes positively charged and, thus adsorbs a counter ion (PF_6^- from TBAH supporting electrolyte) from solution causing the ΔF to decrease,[19] which is actually a contribution of the insertion of the counter ion into the film and also due to film deposition. Then upon dedoping (0 V), the polymer film returns to its neutral state, which ejects the counter ion back to the bulk solution.[19] This makes the ΔF to slightly increase and then plateau. The overall electrodeposition of the polythiophene film onto the QCM crystal is evidenced by the net decrease in ΔF (ca. –365 Hz) after 10 CV cycles. A similar EC-QCM data (Figure S2, SI) is observed with the NIP film (control) deposition onto the PS- (500 nm size) coated Au QCM crystal. However, the NIP electropolymerization shows a greater current response as compared to the MIP film deposition. It is possible that the analyte may have obstructed the inter chain electron transport during the MIP electropolymerization, and thus its current (or also conductivity) is relatively lower than the non-imprinted film.

To confirm the electrodeposition of polythiophene film and imprinting of (–)-norephedrine onto the substrate surface, high resolution X-ray photoelectron spectroscopy (XPS) analysis was performed onto the molecularly imprinted film (after PS removal before template washing). The appearance of the strong sulfur 2p doublet peak between 163.0 and 166.0 eV in **Figure 2**a proves the formation of the polythiophene film onto the substrate.[8] The emergence of the nitrogen 1s peak[8] between 399.0 and 403.0 eV in Figure 2b indicates the successful entrapment of the template molecule in the polymer film. It is important to note that the nitrogen peak is a unique elemental marker for norephedrine. Additional XPS peaks like the carbon 1s between 284.0 and 290.0 eV (Figure 2c) and oxygen 1s between 530.0 and 535.0 eV (Figure 2d) provide supporting evidence of the formation of the molecularly imprinted film. The C 1s peak with the highest intensity located at ~284.8 eV is assigned to the C–C and C–H moieties[19b] while the small shouldering peaks at ~286.0 and ~286.9 eV are attributed to the C=C–S (also C–N from the template) and C=O moieties, respectively.[11c,19b] The small peak at ~289.1 eV in the carbon 1s spectrum is ascribed to the O–C=O functional group of the polythiophene.[19b]

The morphology of the highly ordered and closely packed monolayer assembly of the PS colloidal particle template onto the substrate was determined by atomic force microscopy

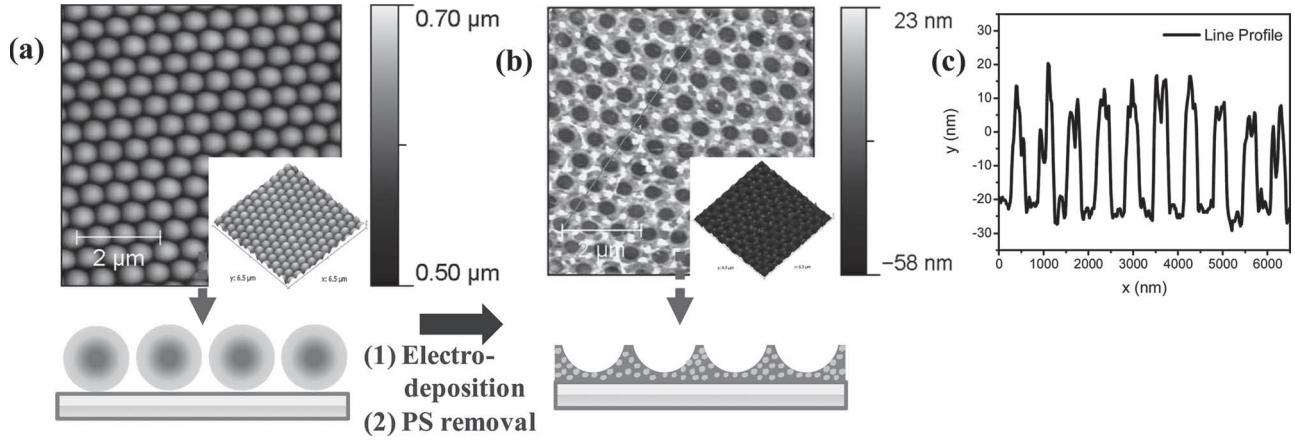

Figure 3. a,b) AFM 2D topography images (3D on inset) of the a) PS-coated substrate and b) molecularly imprinted and templated surface before norephedrine removal with c) its line profile. Note: AFM scan area is 6.5 μm × 6.5 μm. See SI for colored figures.

(AFM). **Figure 3**a shows the 2D ordering of the latex particles in hexagonal arrangement. The monolayer ordering of spherical nanoparticles had been previously reported to be dependent on the vertical withdrawing speed of the LB-like technique and the concentration of the nanoparticles and surfactant (sodium *n*-dodecyl sulfate or SDS) in solution.[10] The same AFM image was observed after the electrodeposition of the MIP film, which indicates that the employed electropolymerization conditions have not disrupted the PS ordering and have enabled controlled electrodeposition of the MIP film at the interstitial void spaces underneath and in between the PS sacrificial template layer. This was verified by the AFM image taken of the imprinted film after washing the colloidal spheres with THF, which leaves behind a highly ordered inverse colloidal array of MIP film (Figure 3b). From the AFM line profile (Figure 3c), the average height of the cavity wall is between ~30 and ~40 nm.

Subsequently after removing the PS sacrificial templates, the imprinted analyte (–)-norephedrine was immediately removed from the nanostructured MIP film via potential induced washing in ethanol and acetonitrile mix solvents (1:1 vol. ratio). To our knowledge, this is the first report of molecular imprinting onto a highly ordered inverse colloidal crystal and nanopatterned electropolymerized polymer array with chiral selectivity. The innovative washing method that involves applying a constant positive potential (at 0.4 V) has been earlier reported by our group for effectively removing different imprinted drugs from planar MIP films. Consistent with our previous results,[8,9] the nanostructured MIP that underwent the constant potential washing had a much higher sensing response (~3-fold decrease in ΔF) upon rebinding of (–)-norephedrine as compared to performing the normal solvent washing with the same solvents (Figure S3, SI). This result can be explained in that more templates were removed from the film by employing the potential wash method, creating more cavities, which influenced later rebinding and sensing properties. As such, this washing method has been consistently adopted.

To test for chiral selectivity, its isomer (+)-norephedrine was injected onto the nanostructured (–)-norephedrine imprinted MIP. From the QCM results (**Figure 4**a), the imprinted film was highly selective towards the imprinted analyte (–)-norephedrine as shown by about three-fold decrease in the change in frequency over the sensing response for the (+)-norephedrine. To confirm its high selectivity, an MIP imprinted film with the reverse template (+)-norephedrine was prepared following exactly the same procedure. Upon injecting (–)-norephedrine onto (+)-imprinted MIP, a much lesser sensing response (denoted by higher ΔF) was also observed as compared to when sensing the imprinted molecule (+)-norephedrine (Figure 4b). These results therefore confirm the high selectivity of the fabricated nanostructured MIP film and the ability to differentiate diastereomers. Naproxen and dopamine were also injected onto the (–)-norephedrine imprinted film (Figure S4, SI), and the MIP film shows limited sensing response to these molecules, which is due to non-specific binding. Furthermore, the sensitivity of the sensor film was validated by injecting different concentrations of the analyte (–)-norephedrine. A calibration plot was constructed on Figure 4c, which displays a linear response (R = 0.978) between 50 to 250 μM analyte concentration. As a control, the same experiment was performed with the NIP film that did not show a linear sensing response. Also, the NIP film showed a lower sensing response (denoted by higher ΔF change), which is attributed to the non-specific binding and adsorption of the template analyte. Finally, to prove the importance of a nanostructured MIP arrayed film prepared with the PS sacrificial colloidal templates, the imprinting of (–)-norephedrine was also done on planar MIP film without the templating. From the QCM results (Figure 4d), the nanostructured MIP demonstrated a significantly higher sensing response (or much lower ΔF) as compared to the planar or non-PS-templated MIP upon (–)-norephedrine rebinding. This implies that the structuring of the surface greatly improved the sensing of the MIP material because of the increase in surface area and possible formation of more cavities easily accessible for template rebinding.

In conclusion, a nanostrutured colloidally templated and electropolymerized MIP film was fabricated for the sensing and high discrimination of a chiral compound and prohibited drug (–)-norephedrine (1*R*, 2*S*) over its diastereomer (+)-norephedrine (1*S*, 2*S*) and vice versa using a facile

NANO MICRO small

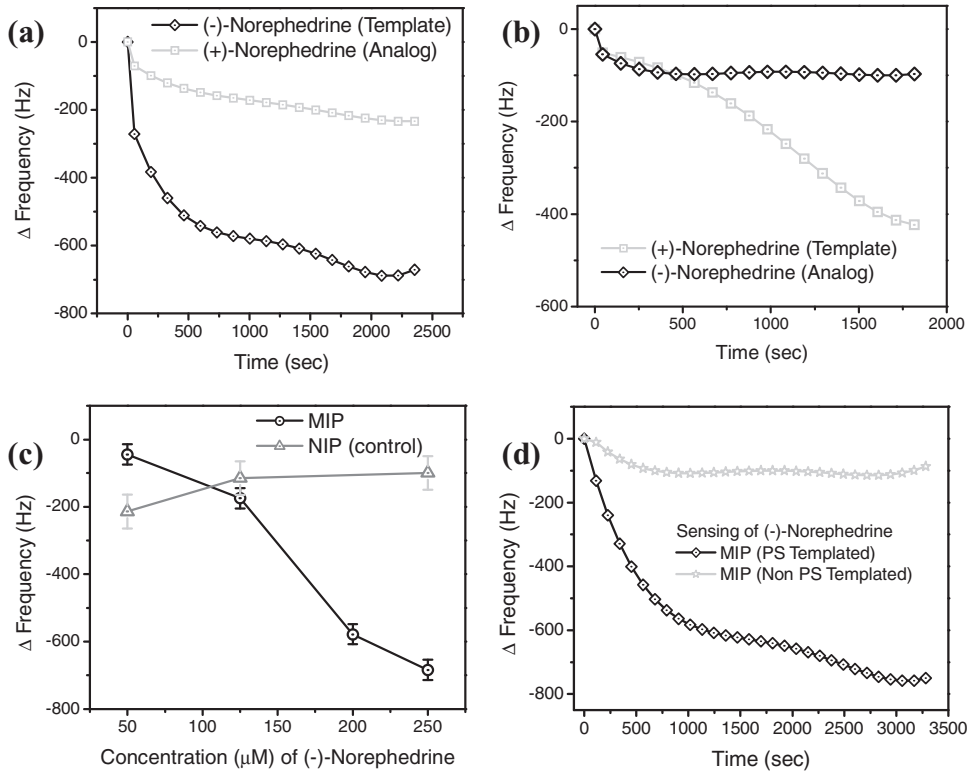

Figure 4. QCM in-situ rebinding studies: QCM sensing of 250 μM concentration of a) (–)-norephedrine (template) versus (+)-norephedrine (analog) and b) (+)-norephedrine (template) versus (–)-norephedrine (analog) (reverse order of imprinting using the same monomer). c) (–)-Norephedrine sensing calibration plot of the MIP film versus the NIP (control) and d) comparison of the sensing response (norephedrine in 250 μM conc.) of the PS and non-PS-templated MIP film. Note: Set-up used was the portable QCM in Figure S1a, SI.

protocol combining the technique of molecular imprinting and colloidal sphere layering via LB-like technique. The new assembly of electropolymerized MIP film had demonstrated a much higher sensing response upon template rebinding than the conventional non-templated and flat MIP film as observed in QCM in-situ measurements. AFM revealed the formation of highly ordered molecularly imprinted and nanopatterned polythiophene film. XPS analysis confirmed the imprinting of the norephedrine as evidenced by the appearance of the strong nitrogen 1s peak that is a unique elemental marker of the template analyte. The appearnace of sulfur 2p peak validated the formation of the polythiophene film. In principle, by utilizing the same fabrication protocol, other bigger templates can also be imprinted like proteins, which are difficult to rebind onto planar MIP films because of steric effects that are imposed by their bulky structure. This work is currently being pursued by our group.

Experimental Section

Materials: The chemicals used were purchased from Sigma-Aldrich except for the terthiophene monomer with carboxylic acid functional group (2-(2,5-di(thiophen-2-yl)thiophen-3-yl)acetic acid abbreviated as G0-3TCOOH), which was synthesized by a modified procedure reported previously (Scheme S1, SI).[20] The details of the synthesis and their NMR spectra (Figure S5, S6, and S7, SI) are found in the SI. A monomer-to-template ratio of 2:1 molar ratio was used in making the MIP film. This optimum ratio was determined from the theoretical modeling studies (Scheme 1, top inset figure). The MIP solution was prepared by mixing the G0-3TCOOH (monomer, 1 mM concentration) with norephedrine (template, 0.5 mM concentration) in acetonitrile (ACN) with 0.1 M tetrabutylammonium hexafluorophosphate (TBAH). The non-imprinted polymer (NIP) solution was prepared in the same manner but without the addition of the template. Note that the MIP solution was prepared for at least 12 h prior to electropolymerization to allow the complexation between monomer and template molecule. For sensing experiments, the solutions of (–)-norephedrine and its isomer (+)-norephedrine were prepared in ACN solution.

MIP Film Fabrication: The layering of PS microbeads was accomplished using a similar procedure described by Grady and co-workers.[10] Briefly, the QCM crystal was attached into the dipper motor via Teflon clip and was dipped into an aqueous solution of PS particles (1 wt.%) and SDS (34.7 mM) as spreading agent. The substrate was withdrawn vertically from the SDS-PS solution at a lift-up rate between 0.1 and 0.3 mm/min. Afterwards the substrate was air dried for a few minutes.

After PS layering, the MIP film was electrodeposited onto the PS-coated Au QCM crystal via CV. The potential was scanned between 0 and 1.1 V at 100 mV/s for 10 CV cycles. After the electrodeposition, the resulting film was washed with ACN thrice to remove the excess monomer. The template analyte was removed from the polymer film via constant potential wash[8,9] in ethanol and ACN solvent mixture (1:1, vol. ratio). Finally, the PS sacrificial templates were removed

from the surface after electropolymerization by dipping the PS-coated substrate in THF twice for 30 minutes.

Instrumentation: CV was performed on an Amel 2049 Potentiostat and Power Lab system (Milano, Italy) containing a three-electrode cell with platinum wire as the counter electrode and Ag/AgCl wire as the reference electrode. The QCM apparatus, probe, and crystals (Figure S1b, SI) were made available from INFICON, Inc. The AT-cut polished QCM crystals (5 MHz) with 1 inch diameter was used as the working electrode. The data acquisition was done with an R-QCM system equipped with a built-in phase lock oscillator and the R-QCM Data-Log software. The portable QCM set-up (QCM 200) used for sensing (Figure S1a, SI) was obtained from Stanford Research Systems (SRS). AFM measurements were done on a Pico-Scan 2500 AFM from Agilent Technologies using tapping mode with scanning rate between 1 and 1.5 lines/s. Commercially available tapping mode tips (TAP300-10, silicon AFM probes, Tap 300, Ted Pella, Inc) were used on cantilevers with a resonant frequency in the range of 290–410 kHz. All AFM topographic images were filtered and analyzed using the Gwyddion software (version 2.19). XPS measurements (at take off angle of 45° from the surface) were carried out on a PHI 5700 X-ray photoelectron spectrometer with a monochromatic Al Kα X-ray source ($h\nu$ = 1486.7 eV) incident at 90° relative to the axis of a hemispherical energy analyzer. Electron binding energies were calibrated with respect to the carbon 1s peak at 284.8 eV. The peaks were analyzed first by background subtraction using the Shirley routine.

Supporting Information

Supporting Information is available from the Wiley Online Library or from the author.

Acknowledgements

The authors would like to acknowledge funding from NSF DMR-10-06776 (colloidal templating part) and CBET-0854979 (sensing part). The authors also acknowledge the generous support of INFICON, Inc. (NY, USA) for providing the Maxtek QCM set-up and QCM crystals.

[1] a) R. C. Advincula, *Korean J. Chem. Eng.* **2011**, *28*, 1313; b) C. Alexander, H. S. Andersson, L. I. Andersson, R. J. Ansell, N. Kirsch, I. A. Nicholls, J. O'Mahony, M. J. Whitcombe, *J. Mol. Recognit.* **2006**, *19*, 106.
[2] M. V. Polyakov, *Zhur. Fiz. Khim.* **1931**, *2*, 799.
[3] a) R. J. Ansell, D. Kriz, K. Mosbach, *Curr. Opin. Biotechnol.* **1996**, *7*, 89; b) D. Spivak, M. A. Gilmore, K. Shea, *J. Am. Chem. Soc.* **1997**, *119*, 4388; c) G. Wulff, *Chem. Rev.* **2002**, *102*, 1.
[4] D. C. Apodaca, R. B. Pernites, R. Ponnapati, F. Del Mundo, R. C. Advincula, *ACS Appl. Mater. Interfaces* **2011**, *3*, 191.
[5] D. C. Apodaca, R. B. Pernites, R. Ponnapati, F. Del Mundo, R. C. Advincula, *Macromolecules* **2011**, *44*, 6669.
[6] D. C. Apodaca, R. B. Pernites, F. Del Mundo, R. C. Advincula, *Langmuir* **2011**, *27*, 6768.
[7] D. Pampa, R. B. Pernites, C. Danda, R. C. Advincula, *Macromol. Chem. Phys.* **2011**, *212*, 2439.
[8] R. B. Pernites, R. Ponnapati, R. C. Advincula, *Macromolecules* **2010**, *43*, 9724.
[9] R. B. Pernites, R. Ponnapati, M. J. Felipe, R. C. Advincula, *Biosens. Bioelectron.* **2011**, *26*, 2766.
[10] M. Marquez, B. P. Grady, *Langmuir* **2004**, *20*, 10998.
[11] a) R. B. Pernites, E. Foster, M. J. Felipe, M. Robinson, R. C. Advincula, *Adv. Mater.* **2011**, *23*, 1287; b) R. Pernites, A. Vergara, A. Yago, K. Cui, R. Advincula, *Chem. Commun.* **2011**, *47*, 9810; c) R. Pernites, R. Ponnapati, R. Advincula, *Adv. Mater.* **2011**, *23*, 3207; d) R. B. Pernites, C. M. Santos, M. Maldonado, R. Ponnapati, D. F. Rodrigues, R. Advincula, *Chem. Mater.* **2011**, DOI: 10.1021/cm2007044.
[12] D. Batra, K. J. Shea, *Curr. Opin. Chem. Biol.* **2003**, *7*, 434.
[13] a) L. Schwarz, C. I. Holdsworth, A. McCluskey, M. C. Bowyer, *Aust. J. Chem.* **2004**, *57*, 759; b) L. Schwarz, M. C. Bowyer, C. I. Holdsworth, A. McCluskey, *Aust. J. Chem.* **2006**, *59*, 129.
[14] B. D. Lindsay, *Mayo Clin. Proc.* **2002**, *77*, 7.
[15] Food and Drug Administration. *Fed. Regist.* **2004**, *69*, 6787.
[16] R. A. Niemann, M. L. Gay, *J. Agric. Food Chem.* **2003**, *51*, 5630.
[17] P. Taranekar, T. Fulghum, D. Patton, R. Ponnapati, G. Clyde, R. Advincula, *J. Am. Chem. Soc.* **2007**, *129*, 12537.
[18] J. Roncali, *Chem. Rev.* **1992**, *92*, 711.
[19] a) B. Deore, Z. Chen, T. Nagaoka, *Anal. Sci.* **1999**, *15*, 827; b) R. B. Pernites, M. J. L. Felipe, E. L. Foster, R. C. Advincula, *ACS Appl. Mater. Interfaces* **2011**, *3*, 817; c) A. G. MacDiarmid, *Angew. Chem., Int. Ed.* **2001**, *40*, 2581.
[20] P. Taranekar, T. Fulghum, A. Baba, D. Patton, R. C. Advincula, *Langmuir* **2007**, *23*, 908.

Received: November 4, 2011
Revised: December 6, 2011
Published online: March 21, 2012

